Laser Physics Letters

LETTER

Investigation of $6S_{1/2}$–$8S_{1/2}$ two-photon transition of cesium atoms by a single 822 nm laser

To cite this article: Ning Liu *et al* 2022 *Laser Phys. Lett.* **19** 025201

IOP Publishing | Astro Ltd Laser Physics Letters
Laser Phys. Lett. **19** (2022) 025201 (5pp) https://doi.org/10.1088/1612-202X/ac3b43

Letter

Investigation of $6S_{1/2}$–$8S_{1/2}$ two-photon transition of cesium atoms by a single 822 nm laser

Ning Liu[1,2], Sandan Wang[1,2], Jinpeng Yuan[1,2,*], Lirong Wang[1,2,*], Liantuan Xiao[1,2] and Suotang Jia[1,2]

[1] State Key Laboratory of Quantum Optics and Quantum Optics Devices, Institute of Laser Spectroscopy, Shanxi University, 92 Wucheng Road, Taiyuan 030006, People's Republic of China
[2] Collaborative Innovation Center of Extreme Optics, Shanxi University, 92 Wucheng Road, Taiyuan 030006, People's Republic of China

E-mail: yjp@sxu.edu.cn and wlr@sxu.edu.cn

Received 3 November 2021
Accepted for publication 16 November 2021
Published 16 December 2021

Abstract

We experimentally investigate the $6S_{1/2}$–$8S_{1/2}$ two-photon transition in cesium vapor by a single laser. A blue (455.5 and 459.3 nm) fluorescence signal is observed as a result of 822.5 nm laser beams illuminating the Cs vapor with a counter-propagating configuration. The dependences of the fluorescence intensity on the polarization combinations of the laser beams, laser power and vapor temperature are studied to obtain optimal experimental parameters. The frequency difference between the two hyperfine components of 4158 (7) MHz is measured with a Fabry–Perot interferometer as a frequency reference. Such a large spectral isolation and the insensitivity to the Earth's magnetic field enable the $6S_{1/2}$–$8S_{1/2}$ transition to be a stable frequency standard candidate for a frequency-doubled 1644 nm laser in the *U*-band window for quantum telecommunication.

Keywords: two-photon transition, fluorescence intensity, frequency standard

(Some figures may appear in color only in the online journal)

1. Introduction

Two-photon transition in atoms is the research foundation of atomic physics and laser physics [1], which provides a convenient ground for rigorous examination of the characteristics of atoms and their interaction with the radiation field [2–4]. Alkali atoms have hydrogen-like atom structure, and are considered an excellent ideal model for spectroscopic research [5]. The study of two-photon transition in alkali atoms, generated in special frequency bands [6, 7], has led to many valuable applications including frequency standard [8–10], quantum telecommunication [11, 12] and other optical technology [13–15].

The $6S_{1/2}$–$8S_{1/2}$ two-photon transition in Cs atoms has attracted tremendous attention for several reasons. For example, ^{133}Cs is the only naturally occurring isotope. Furthermore, *S*–*S* transition can avoid spectral shifting and broadening schemes due to the Zeeman effect [16]. In addition, the hyperfine transition of cesium $6S_{1/2}$–$8S_{1/2}$ possesses large spectral isolation (>4 GHz separation) [17]. More importantly, the two-photon transitionspectrum has narrower linewidth compared to single-photon transition spectrum, and the two-photon transition located at 822 nm can provide a frequency standard candidate for a frequency-doubled 1644 nm laser in the *U*-band window for quantum telecommunication [18].

* Authors to whom any correspondence should be addressed.

Most ^{133}Cs $6S_{1/2}$–$8S_{1/2}$ two-photon transitions are realized by two-color laser beams with a real energy level [19, 20]. Compared to the two-color method, the one-color $6S$–$8S$ two-photon transition system with a virtual energy level is not only more beneficial to device integration, but able to eliminate the Doppler background [21, 22]. However, the low transition probability makes the realization of this process challenging. Although, the frequency comb is employed for the $6S_{1/2}$–$8S_{1/2}$ two-photon transition frequency standard due to its many deterministic frequency components and long-term stability [23, 24], the complicated system prevents its widespread use. Therefore, ^{133}Cs $6S_{1/2}$–$8S_{1/2}$ two-photon transition with an easy-to-implement system is still required for further deeper and more detailed exploration of integrated frequency standards.

In this study, we investigate the spectrum of $6S_{1/2}$–$8S_{1/2}$ two-photon transition excited by a single 822.5 nm laser in thermal Cs atoms. The 455.5 and 459.3 nm fluorescence is clearly observed as the product of two-photon transition. Moreover, the effects of the laser beam polarization combinations, laser power and vapor temperature on the fluorescence intensity are investigated. The relationship between these parameters and the fluorescence intensity revealed in the experiment is consistent with the theory. In this study, we contribute to a valid atomic data supplement of $6S_{1/2}$–$8S_{1/2}$ transition and also provide an excellent experimental platform for building up a stable frequency standard in the U-band window of quantum telecommunication [25].

2. Experiment setup

The energy-level diagram for ^{133}Cs $6S_{1/2}$–$8S_{1/2}$ transition is shown in figure 1(a). The transition wavelength from the ground state ($6S_{1/2}$) to the intermediate state ($6P_{3/2}$) is 852.3 nm, while that from the intermediate state to the excited state ($8S_{1/2}$) is 794.6 nm. Another selectable path is for atoms to be excited from the $6S_{1/2}$ ground state to the $8S_{1/2}$ state via a virtual state, which is indicated by a dotted line in figure 1(a) that represents two 822.5 nm laser beams. The $8S_{1/2}$ excited state atoms will decay back to the $6S_{1/2}$ state via two pathways with radiating 455.5 and 459.3 nm fluorescence. The first is spontaneous radiation to the $7P_{3/2}$ state and then to the $6S_{1/2}$ ground state with 455.5 nm fluorescence, while the second is spontaneous radiation to the $7P_{1/2}$ state and then to the $6S_{1/2}$ ground level with 459.3 nm fluorescence. As a result, the probability of $6S_{1/2}$–$8S_{1/2}$ two-photon transition can be well characterized by the fluorescence intensity.

Figure 1(b) displays the experimental scheme of ^{133}Cs $6S_{1/2}$–$8S_{1/2}$ transition. The 822.5 nm laser is provided by a Ti:sapphire laser system (SolaTis-SRX-XF, M Squared Lasers). The laser wavelength can be tuned in the range of 600–1000 nm and possesses a typical linewidth of less than 1 MHz. The combination of a half-wave plate and a polarizing beam splitter (PBS) is used to divide the laser beam into reflected and transmitted beams. The reflected beam is sent to the Fabry–Perot interferometer (FPI) with a free spectral region of 750 MHz to provide a frequency reference. The transmitted beam interacts with Cs atoms in a vapor cell with a diameter of 2.5 cm and a length of 5 cm. The vapor temperature is accurately adjusted by a temperature controller with a self-feedback system. The transmitted laser beam is retroreflected by a high-reflection mirror (M) to ensure that two counterpropagating laser beams overlap in the cell. Two lenses with a focal length of 20 cm (L_1 and L_2) are used to ensure that the waist of the focused laser beams in the middle of the cell is $\sim$100 μm. The 455.5 and 459.3 nm fluorescence is first focused by two lenses with a focal length of 7.5 cm (L_3 and L_4) and then detected by a photomultiplier tube (Hamamatsu PMT CR131). An interference filter with a center wavelength of 457 nm and a 10 nm pass band (FL457.9–10, Thorlabs) is used to resist the background noise caused by the scattered light.

3. Results and discussions

Fluorescence as the frequency detection of laser is collected by PMT. This is illustrated as a black line in figure 2, when the laser power is 180 mW and the vapor temperature is 480 K. Both forward and retro-reflected 822.5 nm laser beams have linear polarizations. The two-photon transition between the S states requires $\Delta F = 0$ and $\Delta m_F = 0$, where F is the total angular momentum of two photons absorbed by an atom and m_F is its z-component [26]. Therefore, two hyperfine components of the $6S_{1/2}$–$8S_{1/2}$ transition are observed: ^{133}Cs $6S_{1/2}$ ($F = 4$)–$8S_{1/2}$ ($F'' = 4$) and ^{133}Cs $6S_{1/2}$ ($F = 3$)–$8S_{1/2}$ ($F'' = 3$). Since the energy difference between the hyperfine levels is negligible compared to the transition energy between $6S_{1/2}$ and the $8S_{1/2}$, the weight factor is equivalent to the degeneration ($2F + 1$) of the respective hyperfine levels [27]. Here, the experimental valuated ratio of two hyperfine components is in good agreement with the theoretical value of 9:7.

A cavity transmission signal labeled as a red line in figure 2 from an FPI with a 750 MHz free spectral region, is used as a frequency reference to measure the frequency difference between hyperfine components. The frequency difference between the two hyperfine components is 4158 (7) MHz, which is consistent with the previous report of the absolute frequency measurement of Cs $6S_{1/2}$–$8S_{1/2}$ two transition [28]. Such a large spectral isolation between the two hyperfine components (>4 GHz separation) adds a stable background and is also beneficial for providing a frequency standard for the telecommunication of the U-band window [17, 18].

The intensities of the 455.5 and 459.3 nm fluorescence, as products of ^{133}Cs $6S_{1/2}$–$8S_{1/2}$ two-photon transition, are proportional to the population of the $8S_{1/2}$ state. Three experimental parameters, the polarization combinations of the laser beams, the laser power and vapor temperature play a crucial role in the probability of two-photon transition, which directly determine the $8S_{1/2}$ state population.

The selection rule for the Zeeman sublevels in two-photon transitions between the S levels is $\Delta m_F = 0$. Hence, the total angular momentum of two photons absorbed by an atom must be zero. Therefore, only two laser beam polarization combinations satisfy this transition condition. One is the combination of two linearly polarized beams (π–π), while the other is

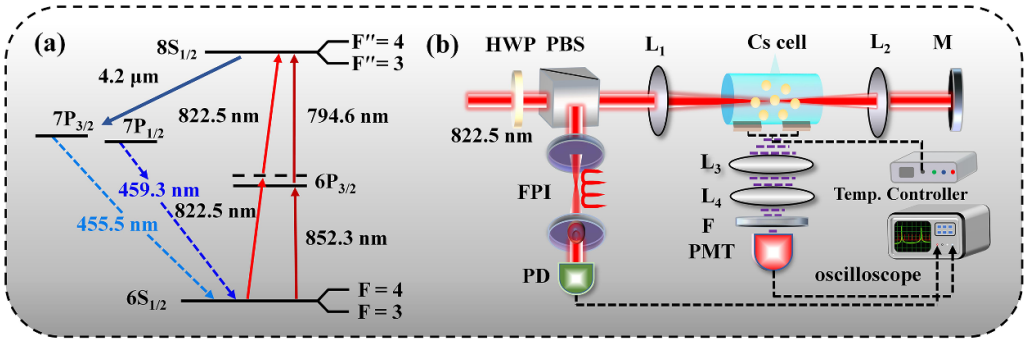

Figure 1. (a) Energy-level diagram of ^{133}Cs $6S_{1/2}$–$8S_{1/2}$ transition. (b) Schematic view of the experimental setup. L, lens; M, high-reflection mirror; QWP, quarter-wave plate; PBS, polarizing beam splitter; FPI, Fabry–Perot interferometer; PMT, photomultiplier tube; F, interference filter; PD, photodetector.

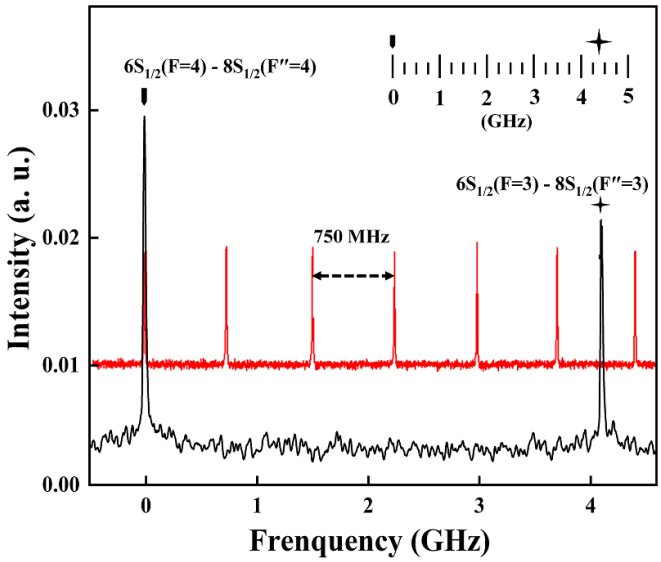

Figure 2. Fluorescence intensity of ^{133}Cs $6S_{1/2}$–$8S_{1/2}$ (black line) transition and FP cavity transmission signal (red line).

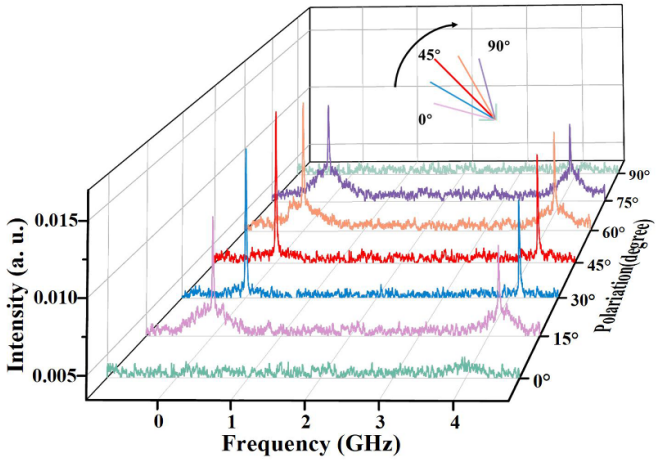

Figure 3. Fluorescence intensity of ^{133}Cs $6S_{1/2}$–$8S_{1/2}$ transition versus the polarization combinations of the laser beams.

the combination of two different-handedly circularly polarized beams (σ^+–σ^-) [27, 29]. The π–π polarization combination is used in this study, while the σ^+–σ^- polarization combination is discussed here. The fluorescence intensity with different polarization angles of the retro-reflected beam is shown in figure 3, while the other experimental parameters are the same as in figure 2. Two QWPs are inserted at each end of the Cs vapor cell to control the polarization combinations of the laser beams. The first is located in the path of the laser beam before the Cs vapor cell to generate a circularly polarized beam. The other is located between the vapor cell and the mirror (M) to control the polarization of the retro-reflected beam.

We record the fluorescence spectrum when the polarization of the retro-reflected beam is changed from 0° to 90° with 15° intervals, as shown in figure 3. When the counter-propagating beams are oppositely circularly polarized (QWP = 45°), the fluorescence intensity reaches the maximum value. The fluorescence intensity reaches the minimum value when the beams have the same polarization (QWP = 0° and 90°). In this situation, the total angular momentum of the two photons absorbed by the atoms is non-zero. Therefore, the transition is forbidden [27]. Note that the σ^+–σ^- polarization combination has a low probability of absorbing two photons with opposite spin angular momentum. Thus, the obtained fluorescence intensity is lower than that of the π–π polarization configuration [27, 30].

The relationship of the fluorescence intensity to laser power is shown in figure 4. The laser power increases from 80 to 180 mW when the vapor temperature is set at 480 K. It is clearly shown that the fluorescence intensity increases with an increase in laser power.

For a two-photon transition between the ground state E_i and the highly excited state E_f, which can be induced by the photons $\hbar\omega_1$ and $\hbar\omega_2$ from two fields with the wave vectors $\boldsymbol{k_1}$ and $\boldsymbol{k_2}$, the transition intensity A_{if} can be expressed as [31]:

$$A_{if} \propto \frac{\gamma_{if} I_1 I_2}{\left[\omega_{if} - \omega_1 - \omega_2 - \boldsymbol{v}\cdot(\boldsymbol{k}_1 + \boldsymbol{k}_2)\right]^2 + (\gamma_{if}/2)^2} \times \left| \sum_k \frac{\boldsymbol{D_{ik}}\cdot\hat{\boldsymbol{e}}_1 \cdot \boldsymbol{D_{kf}}\cdot\hat{\boldsymbol{e}}_2}{\omega_{ki} - \omega_1 - \boldsymbol{v}\cdot\boldsymbol{k}_1} + \frac{\boldsymbol{D_{ik}}\cdot\hat{\boldsymbol{e}}_2 \cdot \boldsymbol{D_{kf}}\cdot\hat{\boldsymbol{e}}_1}{\omega_{ki} - \omega_2 - \boldsymbol{v}\cdot\boldsymbol{k}_2} \right|^2. \quad (1)$$

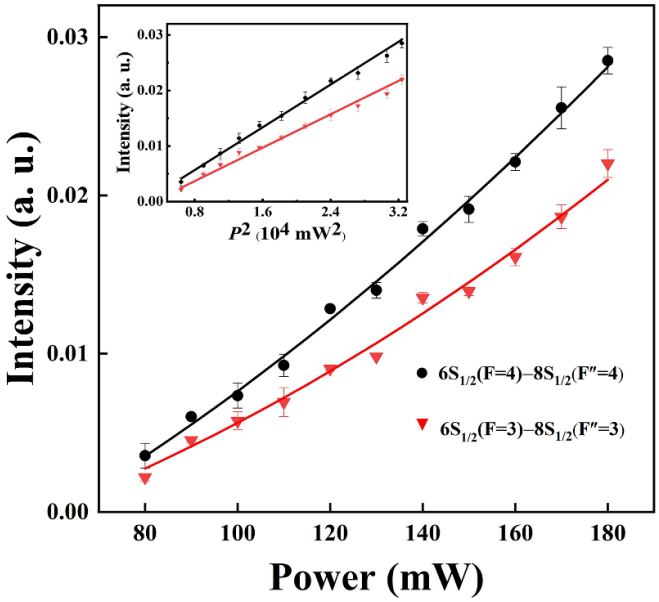

Figure 4. Fluorescence intensity of ^{133}Cs $6S_{1/2}$–$8S_{1/2}$ transition as a function of laser power for linearly polarized beams. Dots represent the experimental results and the solid lines represent the theoretical fittings. Inset shows the relationship between the fluorescence intensity and the laser power square.

The first term represents the spectral-line profile of the two-photon transition, $\boldsymbol{v}$ is the velocity of atoms, γ_{if} is the homogeneous linewidth, and $\widehat{\boldsymbol{e}}_1$ and $\widehat{\boldsymbol{e}}_2$ are the unit vectors along the direction of the axis of quantization for the two laser beams. Here, the quantum axis along the direction of the laser is used to excite the $6S_{1/2}$–$8S_{1/2}$ two-photon transition. I_1 and I_2 are the intensities of the two laser beams. The second term reflects the transition probability of two-photon transition, which can be derived using second-order perturbation theory. D_{ik} is the matrix element for the transitions between the initial state $|i\rangle$ and the intermediate virtual state $|k\rangle$. D_{kf} is the matrix element for the transitions between $|k\rangle$ and the final state $|f\rangle$. For single-color two-photon transition with two counter-propagating laser beams, the laser intensity $I_1 = I_2 = I$, the wave vectors $\boldsymbol{k}_1 = -\boldsymbol{k}_2$, and $\omega_1 = \omega_2 = \omega$. For non-resonant transitions, $\boldsymbol{v}\cdot\boldsymbol{k_i} \ll |\omega_{ki} - \omega_i|$, so $(\omega_{ki} - \omega_i - \boldsymbol{v}\cdot\boldsymbol{k})$ can be approximated by $(\omega_{ki} - \omega_i)$. Therefore, equation (1) can be abbreviated as:

$$A_{if} \propto \frac{\gamma_{if} I^2}{[\omega_{if} - 2\omega]^2 + (\gamma_{if}/2)^2} \times \left| \sum_k \frac{\boldsymbol{D_{ik}}\cdot\widehat{\boldsymbol{e}}_1\cdot\boldsymbol{D_{kf}}\cdot\widehat{\boldsymbol{e}}_2 + \boldsymbol{D_{ik}}\cdot\widehat{\boldsymbol{e}}_2\cdot\boldsymbol{D_{kf}}\cdot\widehat{\boldsymbol{e}}_1}{\omega_{ki} - \omega} \right|^2. \quad (2)$$

The transition intensity increases with increasing laser power and satisfies a quadratic relationship, which is clearly shown in the inset of figure 4 [27]. The ratio of the two fitting curve slopes is 1.279, approaching the theoretical value 9:7. It is noteworthy that when the power increases continuously to above 180 mW, the transition intensity will still increase in theory, but is not discussed here due to limitations of experimental conditions.

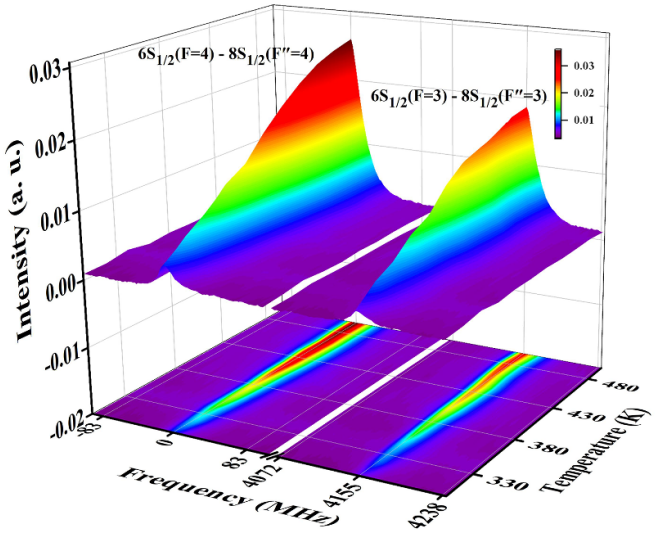

Figure 5. Fluorescence intensity of ^{133}Cs $6S_{1/2}$–$8S_{1/2}$ transition as a function of the vapor temperature.

Figure 5 shows the influence of the vapor temperature on the fluorescence intensity when the laser power is kept at 180 mW. The vapor temperature decreases from 480 to 320 K. It is found that there is continual growth of fluorescence intensity with increasing temperature, and it almost tends to a constant value when the temperature reaches 480 K. The density of the atoms in the cell continuously increases to 2.35×10^{15} cm^{-3} when the vapor temperature increases to 480 K. Nevertheless, when the temperature is over 480 K, slow growth in fluorescence intensity will occur for the $7P_{1/2,3/2}$–$6S_{1/2}$ transition self-absorption effect [32]. Moreover, the linewidth of the Cs $6S_{1/2}$–$8S_{1/2}$ transition spectrum increases with increasing temperature due to the Doppler broadening effect [27].

4. Conclusion

The ^{133}Cs $6S_{1/2}$–$8S_{1/2}$ two-photon transition is demonstrated using a single 822.5 nm laser. The 455.5 and 459.3 nm fluorescence is observed as products of the two-photon transition, which is clear evidence for the transition probability. The frequency difference of 4158 (7) MHz between the two hyperfine components is measured with an FPI. A quadratic relationship between the laser power and fluorescence intensity is also observed, which is consistent with the theoretical prediction. The relationship of fluorescence intensity with combinations of laser beams demonstrates a clear dependence on the law of atomic transition selection rule. In addition, the fluorescence intensity strongly depends on the vapor temperature, which is directly related to the atomic density. The large spectral isolation feature and the insensitivity to the Earth's magnetic field of this transition can provide a frequency standard with a stable background for a frequency-doubled 1644 nm laser in the *U*-band window of quantum telecommunication.

Acknowledgments

The authors gratefully acknowledge the support of the National Natural Science Foundation of China (Grant Nos. 61875112, 62075121 and 91736209), the Program for Sanjin Scholars of Shanxi Province, the Key Research and Development Program of Shanxi Province for International Cooperation (Grant No. 201803D421034) and the Research Project Supported by the Shanxi Scholarship Council of China (Grant No. 2020-073), and 1331KSC.

References

[1] Ficek Z, Seke J, Soldatov A V and Adam G 2001 *Phys. Rev.* A **64** 013813
[2] Simovski C R, Mollaei M S M and Voroshilov P M 2020 *Phys. Rev.* B **101** 245421
[3] Cai H, Liu J H, Wu J Z, He Y Y, Zhu S-Y, Zhang J-X and Wang D-W 2019 *Phys. Rev. Lett.* **122** 023601
[4] Chen Y-H, Liu T-W, Wu C-M, Lee C-C, Lee C-K and Cheng W-Y 2011 *Opt. Lett.* **36** 76
[5] Wu J Z, Xu Y H, Dong R G and Zhang J X 2021 *Opt. Lett.* **46** 3119
[6] Wang S-D, Yuan J-P, Wang L-R, Xiao L-T and Jia S-T 2021 *Front. Phys.* **16** 12502
[7] Park J, Jeong T and Moon H S 2018 *Sci. Rep.* **8** 10981
[8] Glaser C, Karlewski F, Kluge J, Grimmel J, Kaiser M, Günther A, Hattermann H, Krutzik M and Fortágh J 2020 *Phys. Rev.* A **102** 012804
[9] Yuan J P, Liu H, Wang L R, Xiao L T and Jia S T 2021 *Opt. Express* **29** 4858
[10] Hagel G, Nesi C, Jozefowski G L, Schwob C, Nez F and Biraben F 1999 *Opt. Commun.* **160** 1
[11] Walmsley I and Knight P 2002 *Opt. Photonics News* **13** 42
[12] Mangini F, Ferraro M, Zitelli M, Niang A, Tonello A, Couderc V and Wabnitz S 2020 *Phys. Rev.* A **14** 054063
[13] Richter S, Wolf S, Zanthier J and Schmidt-Kaler F 2021 *Phys. Rev. Lett.* **126** 173602
[14] Yuan J P, Li Y H, Li S H, Li C Y, Wang L R, Xiao L T and Jia S T 2017 *Laser Phys. Lett.* **14** 125206
[15] Soumah L, Bossini D, Anane A and Bonetti S 2021 *Phys. Rev. Lett.* **127** 077203
[16] Ko M-S and Liu Y-W 2004 *Opt. Lett.* **29** 1799
[17] Cheng C-Y, Wu C-M, Liao G B and Cheng W-Y 2007 *Opt. Lett.* **32** 563
[18] Lee Y-C, Chui H-C, Chen Y-Y, Chang Y-H and Tsai C-C 2010 *Opt. Commun.* **283** 1788
[19] Perrella C, Light P S, Anstie J D, Baynes F N, White R T and Luiten A N 2019 *Phys. Rev.* A **12** 054063
[20] Sebbag Y, Barash Y and Levy U 2019 *Opt. Lett.* **44** 971
[21] Rajasree K S, Gupta R K, Gokhroo V, Kien F L, Nieddu T, Ray T, Chormaic S N and Tkachenko G 2020 *Phys. Rev. Res.* **2** 033341
[22] Yuan J P, Wu C H, Wang L R, Chen G and Jia S T 2019 *Opt. Lett.* **44** 4123
[23] Martin K W, Phelps G, Lemke N D, Bigelow M S, Stuhl B, Wojcik M, Holt M, Coddington I, Bishop M W and Burke J H 2018 *Phys. Rev.* A **9** 014019
[24] Kim K and Ahn J 2018 *J. Phys.* B **51** 035001
[25] Wu C-M, Liu T-W, Wu M-H, Lee R-K and Cheng W-Y 2013 *Opt. Lett.* **38** 3186
[26] Sasaki K, Sugiyama K, Barychev V and Onae A 2000 *Jpn. J. Appl. Phys.* **39** 5310
[27] Wang S D, Yuan J P, Wang L R, Xiao L T and Jia S T 2019 *Laser Phys. Lett.* **16** 125204
[28] Fendel P, Bergeson S D, Udem T and Hansch T W 2007 *Opt. Lett.* **32** 701
[29] Bonin K D and McIlrath T J 1984 *J. Opt. Soc. Am.* B **1** 52
[30] Nieddu T, Ray T, Rajasree K S, Roy R and Chormaic S N 2019 *Opt. Express* **27** 6528
[31] Antypas D and Elliott D S 2011 *Phys. Rev.* A **83** 062511
[32] Ryan R E, Westling L A and Metcalf H J 1993 *J. Opt. Soc. Am.* B **10** 1643